and Rippel, R. H. (1972), *Biochem. Biophys. Res. Commun. 49*, 863.
Geddes, A. J., Parker, K. D., Atkins, E. D. T., and Beighton, E. (1968), *J. Mol. Biol. 32*, 343.
Lewis, P. N., Momany, F. A., and Scheraga, H. A. (1971), *Proc. Nat. Acad. Sci. U. S. 68*, 2293.
Matsuo, H., Baba, Y., Nair, R. M. G., Arimura, A., and Schally, A. V. (1971), *Biochem. Biophys. Res. Commun. 43*, 1334.
Merrifield, R. B. (1963), *J. Amer. Chem. Soc. 85*, 2149.
Monahan, M., Rivier, J., Burgus, R., Amoss, M., Blackwell, R., Vale, W., and Guillemin, R. (1971), *C. R. Acad. Sci. 273*, 508.
Monahan, M., Rivier, J., Vale, W., Ling, N., Grant, G., Amoss, M., Guillemin, R., Burgus, R., Nicolaides, E., and Rebstock, M. (1972a), *Proc. 3rd Amer. Peptide Symp.*, 601.
Monahan, M. W., and Rivier, J. (1972), *Biochem. Biophys. Res. Commun. 48*, 1100.
Monahan, M. W., Rivier, J., Vale, W., Guillemin, R., and Burgus, R. (1972b), *Biochem. Biophys. Res. Commun. 47*, 511.
Monahan, M. W., Vale, W., Rivier, C., Grant, G., and Guillemin, R. (1973), Abstracts, The Endocrine Society, June.
Némethy, G., and Printz, M. P. (1972), *Macromolecules 5*, 755.
Pauling, L., and Corey, R. B. (1950), *J. Amer. Chem. Soc. 72*, 5349.
Pauling, L., Corey, R. B., and Branson, H. R. (1951), *Proc. Nat. Acad. Sci. U. S. 37*, 205.
Pietta, P. G., and Marshall, G. R. (1970), *Chem. Commun.*, 650.
Vale, W., Grant, G., Amoss, M., Blackwell, R., and Guillemin, R. (1972a), *Endocrinology 91*, 562.
Vale, W., Grant, G., Rivier, J., Monahan, M., Amoss, M., Blackwell, R., Burgus, R., and Guillemin, R. (1972b), *Science 176*, 933.
Venkatachalam, C. M. (1968), *Biopolymers 6*, 1425.
Yamashiro, D. (1964), *Nature (London) 201*, 76.

# Structure of a λ-Type Bence-Jones Protein at 3.5-Å Resolution†

Marianne Schiffer,‡ Rowland L. Girling, Kathryn R. Ely, and Allen B. Edmundson*

ABSTRACT: An electron density map at 3.5-Å resolution has been calculated for a human λ-type Bence-Jones dimer. Organic mercurials, such as *o*-chloromercuriphenol, *p*-hydroxymercuribenzenesulfonate, methylmercuric chloride, and 2-ethylmercurithiosalicylate, were employed to prepare noncovalent isomorphous derivatives. A covalent S–Hg–S derivative, in which a mercury atom was inserted between the sulfur atoms in the interchain disulfide bond in the dimer, was also used to determine the phase angles for the native protein. The dimer is represented by two structural units or "modules." The larger module contains the N-terminal 111 amino acid residues of both monomers and the smaller module consists of the C-terminal 105 residues of the two chains. The amino and carboxyl regions ("domains") of each monomer are connected by an extended chain (the "switch" region). Although the three-dimensional structures of the two monomers are not equivalent, local pseudotwofold axes are found within each module. The axis between the amino domains intersects the axis between the carboxyl domains at an angle of 120°. The amino and carboxyl domains have structural similarities which support the hypothesis of a common ancestral protein. The basic structure of each domain consists of two layers. One layer contains three antiparallel segments of polypeptide chain; the second layer is composed of four segments. An intrachain disulfide bond bridges the two layers in the center of each domain. The three-chain layers in the smaller module (carboxyl domains) supply the outside surface; the four-chain layers provide close contacts at the interface between the two monomers. In an amino domain, the separation of the polypeptide chain into layers is less distinct than in a carboxyl domain. Contrary to expectations, the four-chain layers provide the outer surface of the larger module; the three-chain layers face each other to form a cavity, shaped like a truncated cone 15 Å across at the mouth and 10 Å deep. This cavity, which has many properties attributed to an antigen-binding site of an antibody, is lined by residues from the three "hypervariable" regions of the amino domains. The large side chains of residues 34 and 52 in both monomers protrude into the cavity. The floor of the cavity is composed of an array of four aromatic side chains, two from each monomer. The spatial relations between the amino and carboxyl domains are strikingly different in the two monomers. The evidence suggests that one of the light chains simulates the heavy chain in an antigen-binding (Fab) fragment.

Immunoglobulins are proteins with specific antibody activity or structural features closely resembling those of antibodies. IgG immunoglobulins from myelomatous or normal sera consist of two light (mol wt = 22,000–23,000) and two heavy chains (mol wt = 50,000–55,000). Free light chains excreted into the urine in patients with multiple myeloma are called Bence-Jones proteins, the presence of which can be used as a diagnostic test for the disease (Edelman and Gally, 1962).

We previously reported crystallographic studies of an unusual serum IgG1 immunoglobulin and the urinary λ-type Bence-Jones protein from a patient (Mcg) with multiple myeloma and amyloidosis (Schiffer *et al.*, 1970; Edmundson *et al.*, 1970, 1971, 1972). These proteins were originally isolated and characterized by Deutsch and his colleagues, with whom we are collaborating (Deutsch, 1971; Deutsch and Suzuki,

† From the Division of Biological and Medical Research, Argonne National Laboratory, Argonne, Illinois 60439. *Received July 17, 1973.* This work was supported by the U. S. Atomic Energy Commission.

‡ On leave of absence at the Max Planck Institute for Biochemistry, 8033 Martinsried, Munich, West Germany.

1971; Fett *et al.*, 1973). The heavy chain of the Mcg serum immunoglobulin has a deletion of 15 amino acid residues in the "hinge" region. The deleted region includes the half-cystine residues usually participating in the interchain disulfide bonds between heavy chains and between heavy and light chains. Mcg light chains are of normal length, and the penultimate half-cystine residues, generally connected to the heavy chains, bridge light chain monomers both within the IgG molecule and in the Bence-Jones protein. The proteins from one myeloma patient like Mcg are particularly favorable for comparative structural studies because the light chains and Bence-Jones proteins have the same amino acid sequences.

Within each species and antigenic class, the sequences of the carboxyl halves of light chains are relatively constant (C), while the amino halves vary (V) both in sequence and in length (Hilschmann and Craig, 1965; Titani *et al.*, 1966). Each half contains ~105–112 residues, independently folded into crystallographically distinct regions or "domains" (Edmundson *et al.*, 1972; Poljak *et al.*, 1972; for discussion of the domain hypothesis, see Edelman and Gall, 1969). The chains in the "switch" regions between the two domains are particularly sensitive to proteolytic and acidic hydrolysis (Solomon and McLaughlin, 1969; Karlsson *et al.*, 1969, 1972; Björk *et al.*, 1971; Schramm, 1971).

In antibody molecules, both light and heavy chains contribute to antigen-binding sites (Thorpe and Singer, 1969; Singer *et al.*, 1971; Goetzl and Metzger, 1970; Milstein and Pink, 1970; Cebra *et al.*, 1971; Franěk, 1971; Haimovich *et al.*, 1971, 1972; Porter, 1971; Press *et al.*, 1971; Inbar *et al.*, 1972; Painter *et al.*, 1972a,b; Cathou and Dorrington, 1973). Hypervariable sequences, of which there are three in the light chains (Wu and Kabat, 1970; Kabat and Wu, 1971; Garver and Hilschmann, 1971) and three to four in the heavy chains (Capra, 1971; Capra *et al.*, 1971; Kehoe and Capra, 1971), are believed to be constituents or near neighbors of the binding sites.

Since the sequences of the light and heavy chains are homologous (Singer and Doolittle, 1966; Hill *et al.*, 1966), it is of interest to ask if the Mcg Bence-Jones dimer forms a binding site similar to that in an Fab (antigen-binding) fragment of an antibody molecule. Deutsch (1971) proposed that the Mcg dimer may have antibody-like activity to a lipid or lipoprotein in the subcutaneous tissue encompassing amyloid deposits. In individuals in which multiple myeloma is accompanied by amyloidosis, the Bence-Jones proteins generally have a stronger affinity for tissue components than in patients with multiple myeloma alone (Osserman *et al.*, 1964).

In the present article we describe the structure of the Mcg Bence-Jones dimer at 3.5-Å resolution. Other pertinent crystallographic studies of human immunoglobulins or their fragments include those of an IgG cryoglobulin (Sarma *et al.*, 1971), an Fab fragment consisting of a λ-type light chain covalently linked to the amino half of a heavy chain (Poljak *et al.*, 1972), a κ-type Bence-Jones monomer (Epp *et al.*, 1972), and a V fragment of a κ chain (Solomon *et al.*, 1970). In addition, Padlan *et al.* (1973) are determining the structure of a murine Fab fragment which has a κ-type light chain and antigenic specificity toward phosphorylcholine.

## Materials and Methods

*Properties of the Crystals.* As reported previously (Edmundson *et al.*, 1971, 1972), the Mcg Bence-Jones dimer crystallizes at pH 6.2 from 1.6 M ammonium sulfate in the trigonal space group $P3_121$, with $a$ = 72.3 Å and $c$ = 185.9 Å. The dimer (mol wt = 46,000) is the asymmetric unit.

TABLE I: Final Heavy-Atom Parameters.

| Derivative | Site | $x$ | $y$ | $z$ | $A^a$ | $B^a$ |
|---|---|---|---|---|---|---|
| S–Hg–S I from solution | 1 | 0.111 | 0.542 | 0.110 | 283.7 | 3.3 |
| S–Hg–S II in the crystal | 1 | 0.111 | 0.542 | 0.110 | 284.8 | 4.0 |
| *o*-Chloromercuriphenol (2.0 mM) | 1 | 0.196 | 0.479 | 0.156 | 291.2 | 0.3 |
| | 2 | 0.422 | 0.143 | 0.114 | 390.0 | 3.7 |
| | 3 | 0.608 | 0.259 | 0.157 | 118.2 | 4.9 |
| *o*-Chloromercuriphenol (0.75 mM) | 1 | 0.196 | 0.479 | 0.156 | 192.1 | 1.2 |
| | 2 | 0.423 | 0.143 | 0.115 | 293.6 | 4.6 |
| | 3 | 0.609 | 0.256 | 0.158 | 63.2 | 6.6 |
| *p*-Hydroxymercuribenzenesulfonate (10.0 mM) | 1 | 0.260 | 0.486 | 0.152 | 231.2 | 1.4 |
| | 2 | 0.290 | 0.464 | 0.017 | 75.1 | 5.6 |
| | 3 | 0.335 | 0.506 | 0.129 | 74.6 | 7.9 |
| | 4 | 0.495 | 0.189 | 0.107 | 182.3 | 5.7 |
| | 5 | 0.927 | 0.715 | 0.050 | 60.5 | 4.6 |
| Methylmercuric chloride (saturated) | 1 | 0.208 | 0.479 | 0.154 | 139.8 | 9.8 |
| | 2 | 0.296 | 0.468 | 0.018 | 112.8 | 11.7 |
| | 3 | 0.389 | 0.759 | 0.144 | 114.9 | 15.4 |
| | 4 | 0.430 | 0.843 | 0.107 | 119.9 | 14.8 |
| | 5 | 0.440 | 0.148 | 0.113 | 183.3 | 12.4 |
| | 6 | 0.610 | 0.263 | 0.157 | 102.4 | 6.2 |
| | 7 | 0.722 | 0.530 | 0.123 | 85.5 | 10.0 |
| | 8 | 0.922 | 0.716 | 0.054 | 89.4 | 11.8 |
| Sodium merthiolate (10.0 mM) | 1 | 0.082 | 0.672 | 0.099 | 148.2 | 32.0 |
| | 2 | 0.151 | 0.473 | 0.083 | 257.8 | 15.4 |
| | 3 | 0.405 | 0.780 | 0.146 | 422.2 | 22.0 |
| | 4 | 0.428 | 0.864 | 0.129 | 451.4 | 49.9 |

[a] $A$ = occupancy on an arbitrary scale; $B$ = temperature factor.

*Preparation of Isomorphous Heavy-Atom Derivatives.* Of the two organic mercurials used in the determination of the 6-Å structure, *o*-chloromercuriphenol, but not sodium mersalyl, formed derivatives suitable for studies at higher resolution. Additional noncovalent derivatives were sought by a screening process in which the initial step was an examination of the 00*l* reflections for intensity changes after a 4–6-week soak of a crystal in the appropriate solution. When average changes >20% were observed, a 6.5-Å shell of data was collected and a three-dimensional difference Fourier was calculated, using the protein phases previously determined.

Noncovalent isomorphous derivatives were prepared with sodium 2-ethylmercurithiosalicylate (merthiolate), methylmercuric chloride, *p*-hydroxymercuribenzenesulfonate, *p*-chloromercuriphenol, and mercuhydrin (a complex of theophylline and the sodium salt of methoxyhydroxymercuriopropylsuccinylurea). The first three, together with *o*-chloromercuriphenol at two concentrations (0.75 and 2.0 mM), were used in phasing: sodium merthiolate to 6.5 Å; methylmercuric chloride to 5.0 Å; and *p*-hydroxymercuribenzenesulfonate and *o*-chloromercuriphenol to 3.5 Å (see Table I).

A special procedure was used to prepare the methylmercury derivative. Solid methylmercuric chloride was added past the point of saturation to 1.6 M ammonium sulfate in a 20-ml glass reaction vessel that could be tightly sealed. Crystals of

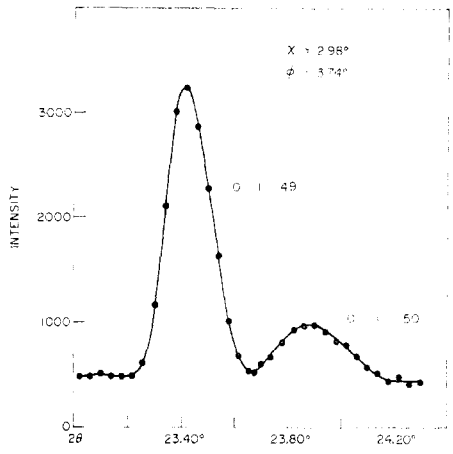


FIGURE 1: The $2\theta$ step scan of two of the most closely spaced reflections in the 3.5-Å shell. The calculated values for the center of each reflection were: for 0, 1, 49, $2\theta = 23.39°$, $\chi = 3.01°$, and $\phi = 3.75°$; for 0, 1, 50, $2\theta = 23.87°$, $\chi = 2.95°$, and $\phi = 3.72°$. The $\chi$ and $\phi$ angles were set to average values. The crystal to detector distance was 52 cm; the take-off angle was 4°; and the receiving aperture was 2 × 4 mm.

protein in ammonium sulfate were placed in a glass cup on a pedestal over the reservoir of the mercurial solution. The upper solution was kept saturated by vapor phase diffusion of the reagent without the presence of solid to obscure observations of the protein crystals during the soak period and during their removal for mounting in quartz capillaries. Solid reagent as well as mother liquor were added to the capillaries to minimize diffusion of the mercurial from the crystal. Because of the toxicity of the reagent, all steps were performed with care in a hood.

A covalent derivative was prepared by reducing the interchain disulfide bond and inserting mercury between the sulfur atoms. The reactions were carried out both in solution, with subsequent crystallization (type I), and by diffusion of reactants into crystals (type II). Details were presented in a previous article (Ely *et al.*, 1973).

*Data Collection and Processing.* Using an $\omega$ step scan (Wyckoff *et al.*, 1967) with an automated Picker four-circle diffractometer, we collected data by the procedure described in the 6-Å study (Edmundson *et al.*, 1972). Because of the long $c$ axis, care was taken to demonstrate resolution of the most closely spaced reflections (*i.e.*, the $01l$ series), as shown in Figure 1. The differences in the angle settings of the two adjacent reflections ($\Delta 2\theta = 0.48°$; $\Delta\chi = 0.06°$; and $\Delta\phi = 0.03°$) indicate that resolution was achieved largely on the basis of $\Delta 2\theta$ values. The separations became greater as the $\Delta\phi$ values increased.

The 3.5-Å sphere contained approximately 7500 reflections, which were collected with three crystals in six concentric shells. Data reduction was carried out as in the 6-Å study, with the exception that reflections with intensities lower than five times their standard deviations were designated as unobserved and removed from the data set for the native protein. The discarded reflections comprised 11.7% of the total, distributed among the shells as follows: infinity to 6.5 Å, 4.0%; 6.5–5.0 Å, 10.0%, 5.0–4.4 Å, 9.6%; 4.4–4.0 Å, 15.3%; 4.0–3.7 Å, 14.4%; 3.7–3.5 Å, 18.1%.

The decay correction for each shell was based on the average decrease in intensity of about 30 reflections selected from the 6.5-Å sphere to have structure factors of 4000–8000, compared to an average value of ~3400 for the entire shell.[1] These reflections from crystals of the native protein were also used to determine the relative scale factors for the combined shells of data. The scale factor ($k$) for each isomorphous derivative was calculated with the expression $\Sigma F_P = k\Sigma F_{PH}$, where $F_P$ and $F_{PH}$ are the structure factor amplitudes of the protein and derivative, respectively. A separate scale factor was calculated for each shell.

These scale factors were used to combine the shells before refinement of the heavy-atom parameters ($x$, $y$, $z$, occupancy, and isotropic temperature factor). The refinement was carried out in the following four steps by the method of alternate cycles of phase determination and least-squares refinement (Dickerson *et al.*, 1968). The parameters were first refined with centric data. All data were then included, using the most probable phases (Adams *et al.*, 1969). The derivative scale factors were next refined by shells. Finally, the refinement of parameters was repeated with all data. The trend toward convergence was evidenced by the small mean shift (0.02 Å) in the positions of the heavy atoms and the small mean change (0.12°) in phase angles of the protein in the last two cycles of refinement. The final coordinates of the heavy-atom derivatives used for phasing are listed in Table I. Results of the refinement procedures and the error analyses are presented in Table II. The average figure of merit for all data was 0.81.

*Enantiomorphic Analysis.* Anomalous dispersion data for the *o*-chloromercuriphenol derivative were collected to distinguish between the two possible enantiomorphic space groups $P3_121$ and $P3_221$. Strong reflections, with a peak to background ratio of ~10:1, were selected by criteria designed to maximize differences in intensity between Friedel pairs (Cullis *et al.*, 1962). In each case, the contribution of the mercury atom was large and the difference in phase angles between the native protein and derivative was 90 ± 50 or 270 ± 50°. Differences in the intensities of 28 of 30 pairs of reflections were consistent with predictions based on the space group $P3_121$.

*Calculation of Electron Density Map.* The electron density map was calculated with "best" phases (Blow and Crick, 1959) and with the observed structure factors weighted by the figure of merit. Sections were computed normal to $a^*$ and printed out on a scale of 2 cm = 1 Å. The grid points were separated by 1.0 Å along $a^*$, 0.846 Å along $b$, and 0.762 Å along $c$. The map was plotted on an arbitrary scale, with up to seven contours in increments of 100; the zero contour was omitted. The standard deviation of the electron density was 87 on this scale (Dickerson *et al.*, 1961). The contours were traced on glass sheets, which were placed in an optical comparator for model building (Richards, 1968).

*Model of the Bence-Jones Dimer.* A model was constructed by fitting AWG 4 plastic-coated electrical wire to the electron density for the polypeptide backbone, as illustrated in Figure 2. To obtain this illustration, the mirror image of the model was photographed on the same film as the electron density.

In the figures monomer 1 is shown as white or grey tubing, and monomer 2 is represented by black tubing. Figures 6, 7, 8a, 12b, and 13 are tracings of photographs of the actual model, with alterations to clarify cross-over points. Figures 9 and 10 are stereo photographs of the V and C domains.

[1] Our current operating programs for data collection include a file system with which we can use reflections throughout the 3.5-Å sphere to obtain decay corrections as a function of $2\theta$. The present method improves the precision of the structure factor values up to about 1.3% for $2\theta$ angles corresponding to 3.5–4.0-Å resolution.

TABLE II: Results of Refinement; Radial Distribution of Mean Values.

| Interplanar spacing in Å ($d$) | All data | 10.45 | 6.28 | 4.87 | 4.12 | 3.66 |
|---|---|---|---|---|---|---|
| Figure of merit ($m$) | 0.81 | 0.92 | 0.86 | 0.82 | 0.78 | 0.71 |
| Average protein structure factor ($F$) | 3242 | 3616 | 2846 | 3658 | 3399 | 2787 |
| No. of reflections ($n$) | 6547 | 790 | 1175 | 1475 | 1605 | 1502 |
| S–Hg–S I from solution | | | | | | |
| $R_F$[a] | 0.106 | 0.147 | 0.130 | 0.090 | 0.091 | 0.101 |
| $R_K$ | 0.061 | 0.071 | 0.062 | 0.051 | 0.058 | 0.074 |
| $f$ | 432 | 563 | 510 | 446 | 387 | 340 |
| $E$ | 199 | 263 | 176 | 183 | 194 | 206 |
| S–Hg–S II in the crystal | | | | | | |
| $R_F$ | 0.105 | 0.132 | 0.121 | 0.094 | 0.105 | 0.089 |
| $R_K$ | 0.063 | 0.052 | 0.055 | 0.060 | 0.074 | 0.063 |
| $f$ | 408 | 558 | 491 | 420 | 356 | 305 |
| $E$ | 205 | 190 | 168 | 220 | 251 | 177 |
| *o*-Chloromercuriphenol (2.0 mM) | | | | | | |
| $R_F$ | 0.198 | 0.219 | 0.228 | 0.188 | 0.184 | 0.188 |
| $R_K$ | 0.115 | 0.081 | 0.114 | 0.114 | 0.123 | 0.129 |
| $f$ | 847 | 1013 | 932 | 846 | 804 | 740 |
| $E$ | 377 | 300 | 335 | 421 | 420 | 364 |
| *o*-Chloromercuriphenol (0.75 mM) | | | | | | |
| $R_F$ | 0.124 | 0.161 | 0.155 | 0.115 | 0.105 | 0.108 |
| $R_K$ | 0.067 | 0.064 | 0.075 | 0.065 | 0.064 | 0.073 |
| $f$ | 540 | 707 | 621 | 543 | 493 | 436 |
| $E$ | 219 | 233 | 212 | 236 | 218 | 201 |
| *p*-Hydroxymercuribenzenesulfonate (10.0 mM) | | | | | | |
| $R_F$ | 0.113 | 0.152 | 0.143 | 0.100 | 0.094 | 0.105 |
| $R_K$ | 0.059 | 0.054 | 0.057 | 0.051 | 0.062 | 0.071 |
| $f$ | 507 | 630 | 564 | 515 | 466 | 433 |
| $E$ | 191 | 196 | 164 | 186 | 207 | 196 |
| Methylmercuric chloride (saturated) | | | | | | |
| $R_F$ | 0.118 | 0.140 | 0.113 | 0.091[b] | | |
| $R_K$ | 0.072 | 0.076 | 0.070 | 0.068 | | |
| $f$ | 417 | 394 | 377 | 280 | | |
| $E$ | 229 | 277 | 200 | 220 | | |
| Sodium merthiolate (10.0 mM) | | | | | | |
| $R_F$ | 0.163 | 0.177 | 0.130[c] | | | |
| $R_K$ | 0.073 | 0.067 | 0.088 | | | |
| $f$ | 659 | 795 | 413 | | | |
| $E$ | 247 | 240 | 260 | | | |

[a] $R_F = \Sigma|F_{PH} - F_P|/\Sigma F_P$; $R_K = \Sigma|F_{PH,obsd} - F_{PH,calcd}|/\Sigma F_{PH,obsd}$, where $F$ = structure factor amplitude; P = protein; H = heavy atom; PH = protein plus heavy atom; $f$ = calculated heavy-atom contribution on an arbitrary scale; $E$ = lack of closure error. [b] $n = 498$; $d = 5.23$. [c] $n = 438$; $d = 7.04$.

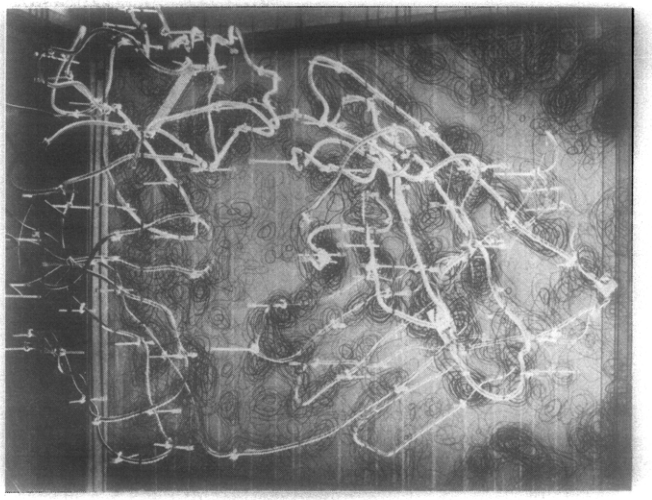

FIGURE 2: Photograph of the mirror image of the protein model superimposed on stacked sections of the 3.5-Å electron density map. This illustrates the fitting of electrical wire to the electron density of the polypeptide backbone.

The positions of the amino acid residues on the polypeptide chains are numbered as in the *Atlas of Protein Sequence and Structure* (Dayhoff, 1972) for the Bo λ chain (Wikler and Putnam, 1970). The positions indicated in the figures are probably accurate to ± one residue.

## Results and Discussion

*Heavy-Atom Derivatives.* Among the organic mercurials listed in Table I, *o*-chloromercuriphenol and *p*-hydroxymercuribenzenesulfonate formed the best derivatives. The results at two concentrations of *o*-chloromercuriphenol were comparable, and no significant differences were observed when *p*-chloromercuriphenol was substituted for the ortho compound.

Like *o*-chloromercuriphenol and mersalyl (Edmundson *et al.*, 1972), other organic mercurials were found mainly in the large module. In the covalent S–Hg–S derivative, the mercury atom marking the interchain disulfide bond was located at the junction of the small module of one molecule and the large module of an adjacent dimer (Ely *et al.*, 1973).

The principal sites of mersalyl, merthiolate, and mercuhydrin were located in the cavity between the two homologous domains in the large module (see Figure 12b; part of the cavity is marked with an asterisk in Figure 3). The major sites of *o*- and *p*-chloromercuriphenol and *p*-hydroxymercuribenzenesulfonate were outside the cavity. Methylmercuric chloride, more compact and volatile than the aromatic compounds, entered eight sites, including the mersalyl and phenolic locations.

The aromatic mercurials also showed overlapping specificity. For example, the two major phenolic sites (no. 1 and 2 in Table I) served as secondary sites for mersalyl and were close to the principal *p*-hydroxymercuribenzenesulfonate sites. It is not possible to define all of the sites in detail until the amino acid sequence is completed, but the two phenolic sites are adjacent to large side chains, one in each domain. In the Bo λ-type Bence-Jones protein (Wikler and Putnam, 1970), a histidine residue is found in the comparable part of the sequence. The presence of histidine is consistent with the specificity of mersalyl, which interacts with the imidazole group in other proteins (*e.g.*, cytochrome *c;* Dickerson *et al.*, 1969).

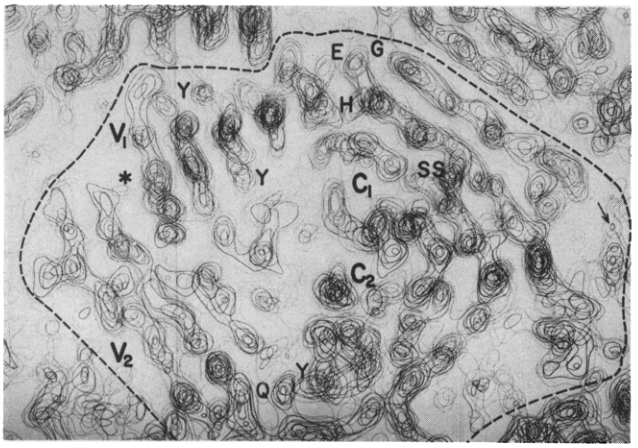


FIGURE 3: Photograph of superposed sections of the 3.5-Å electron density map. Sections are normal to the $a^*$ axis, with $y$ the ordinate and $z$ the abscissa in each section. There are seven contours at intervals of 100; the 100 contour level is shown as a light grey line, and the zero contour is omitted. The molecular boundary of the Bence-Jones dimer is indicated by the dashed line. The variable and constant domains are labeled V and C with the appropriate subscript for monomer 1 or 2. Part of the cavity separating the V domains is marked with an asterisk. Prominent side chains are designated by their one-letter codes. The numbering system in the Bo λ chain (Wikler and Putnam, 1970; see Dayhoff, 1972) is used in all figures, pending completion of chemical sequence studies on the Mcg protein by J. W. Fett and H. F. Deutsch (personal communication). In the $V_1$ domain, the upper and lower tyrosine (Y) side chains represent residues 88 and 89, respectively. In murine anti-dinitrophenyl antibodies, the residue equivalent to tyrosine 88 is susceptible to affinity labeling (see text). Glutamine 112 (Q) is a constituent of the connecting segment ("switch" region) between the V and C domains. The side chains of glutamine 112 and tyrosine 144 are in van der Waal's contact in the $C_2$ domain. The upper two chains in the $C_1$ domain are antiparallel and continuous around the bend formed by histidine 201 (H), glutamic acid 202 (E), and glycine 203 (G). The upper chain is also antiparallel to the C-terminal segment of another Bence-Jones dimer, appearing on the opposite side of the molecular boundary. The arrow from the upper chain points in the general direction of the interchain disulfide bond. The intrachain disulfide bond in the $C_1$ domain is marked SS.

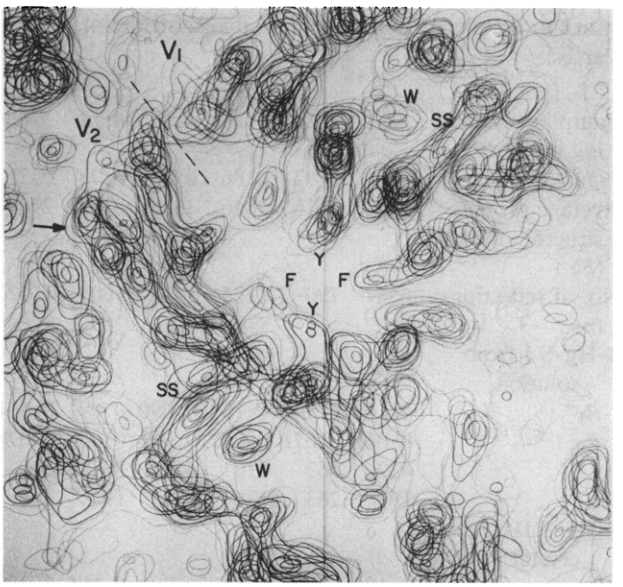


FIGURE 4: Superposed sections of electron density for parts of the V domains. The two intrachain disulfide bonds are represented by the straight segments of high density marked SS. The "invariant" tryptophan side chain (37) on one side of each disulfide bond is labeled W. The four aromatic side chains forming the floor of the cavity between V domains are designated by Y and F, codes for tyrosine and phenylalanine. The arrow marks the start of the turn of the segment which leads from the intrachain disulfide bond through the phenylalanine to connect with the C domain.

The principal sites for mersalyl, mercuhydrin, and merthiolate will be considered in the discussion of the cavity in the large module.

*General Description of Electron Density*. Superposed sections illustrating the quality and features of the 3.5-Å map are shown in Figures 3–5. The large and small modules representing the Bence-Jones dimer were clearly separated from other asymmetric units (see molecular boundary in Figure 3). The modules were bridged by two sections of electron density, one of which is shown at the bottom of Figure 3. Examination of the 3.5-Å map confirmed that the pair of modules used to represent the dimer in the 6-Å model (Edmundson *et al.*, 1972) was the correct choice.

Within each module the boundaries between homologous domains were also clearly defined. The polypeptide backbone of each monomer appeared as a ribbon of electron density continuous throughout practically the entire molecule. There were sections of low density on the surface of the large module near one end of the intrachain disulfide loop in the upper monomer (1) in Figures 6 and 7. However, the corresponding segments were more clearly defined in the lower monomer (2). The redundancy in having different views of the same amino acid sequences was helpful in tracing the chains unambiguously.

The most prominent features of the map were the four intrachain disulfide bonds, which formed straight columns of high electron density (see Figure 4). The density for the interchain disulfide bond in the native protein was substantially lower than that for any intrachain disulfide bridge. This low density can be partly explained by the lack of complete isomorphism at the mercury site in the S–Hg–S derivative (Ely *et al.*, 1973). Moreover, the interchain disulfide bond is on the surface of the molecule and has more freedom to move than the intrachain linkages.

Density corresponding to amino acid side chains emerged from the backbone at regular intervals, except in the glycine positions. The tryptophan residues could be readily identified, and the other aromatic side chains usually had characteristic shapes (see Figures 3–5). As in the study of elastase at 3.5 Å (Shotton and Watson, 1970), the electron density at the α carbon was higher than that in the carbonyl positon.

*Identification of the V, C, and "Switch" Regions*. After the polypeptide chains were followed and attempts were made to fit the known sequence of the C-terminal halves to the electron density, we concluded that the small module contains the C domains of the two monomers. The location of the S–Hg–S marker is consistent with this conclusion.

The difference in size of the two modules is illustrated by the distances between centers of the intrachain disulfide bonds: 24 Å in the $V_1$ and $V_2$ domains, but only 18 Å in the C regions (see Figures 6–8). The size differential is too great to be attributed solely to the numbers of residues in the V (111) and C (105) domains. However, it can be largely explained by the presence of a cavity between the V regions (see later section).

The two segments of electron density bridging the modules correspond to the "switch" regions between the V and C parts of the amino acid sequences. The switch regions were not apparent in the 6-Å map, and the segments which seemed

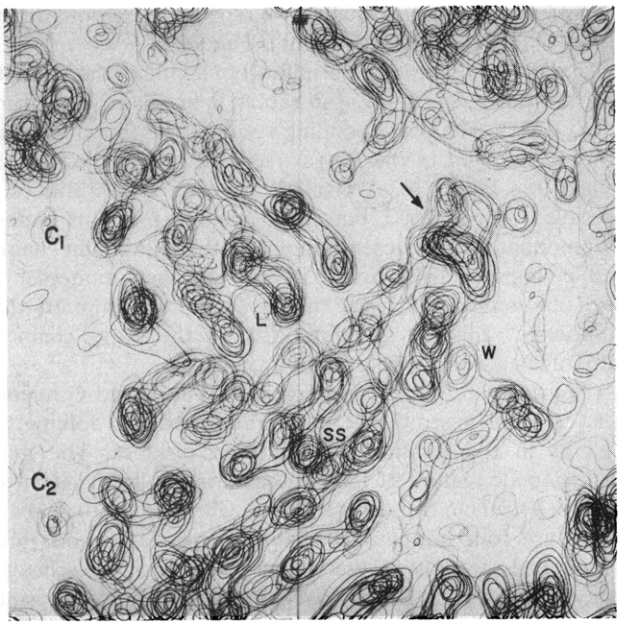


FIGURE 5: Superposed sections of electron density of parts of the C domains. This figure illustrates the diagonal arrangement of chains in the two domains. Leucine 139 (L) is immediately adjacent to the intrachain disulfide bond, which is not shown in $C_1$, but does appear in $C_2$. Both disulfide bonds are located near the faint vertical line drawn at $z = 2/3$. The side chain of tryptophan 189 (W) emanates from a chain below these sections of electron density and seems to interact with part of the C-terminal segment (note connecting density below the letter W). The arrow marks the bend of the loop connecting the intrachain disulfide bond in the $C_2$ region with its counterpart in the $V_2$ region (see segment marked with arrow in Figure 4).

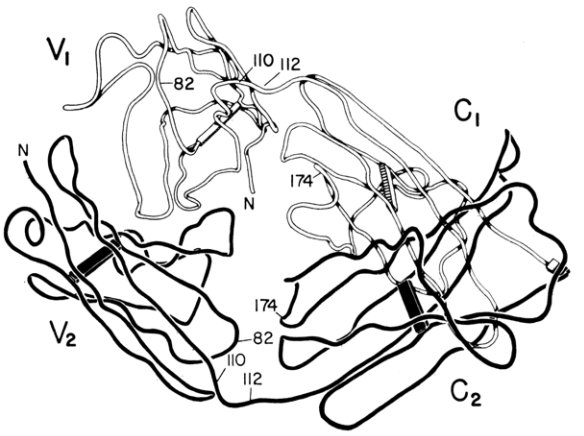


FIGURE 6: Tracing of a photograph of the model of the Bence-Jones dimer with the C domain of monomer 2 facing the camera. Monomer 1 is shown in white and monomer 2 is shown in black. The N-termini are labeled N, and residues of particular interest are indicated by their approximate positions in the amino acid sequence. Leucine 110 is adjacent to the bend in the segment connecting the V and C domains, and glutamine 112 marks the beginning of the sequence usually assigned to the C "half" of a λ chain. Disulfide bonds are represented by bars between appropriate segments. The interchain disulfide bond between the penultimate half-cystine residues is located at the far right. The additional intrachain disulfide bond in rabbit light chains (see text) is formed between residues in positions equivalent to Mcg 82 and 174. The appropriate chains in monomer 2, but not in monomer 1, are sufficiently close for the formation of such a bond.

to connect the modules proved to be close contacts between the V and C regions of monomer 1 (see Figures 6 and 7). The accessibility of the extended chains comprising the switch regions (see Figures 6 and 7) explains the ease with which light chains can be cleaved into V and C domains (Solomon and McLaughlin, 1969; Karlsson *et al.*, 1969, 1972; Björk *et al.*, 1971; Schramm, 1971; Fraser *et al.*, 1972).

*Local Twofold Axes in the Bence-Jones Dimer.* As emphasized in the 6-Å study, the Bence-Jones dimer does not have an axis of symmetry (Edmundson *et al.*, 1972). The 3.5-Å map clearly indicates that the two monomers are not equivalent in their three-dimensional structures, although local pseudo-twofold axes are found between each pair of like domains (see Figures 8a and 8b). These twofold axes intersect at an angle of 120°. The symmetry breaks down for about five residues in the switch regions and for the C-terminal six residues (including the interchain disulfide bond).

In this asymmetric unit, the twofold axis between the V domains makes angles of 40, 70, and 55° with the *a**, *b*, and *c* directions, respectively. It forms an angle of 33° with the "particle axis," which we define as a line through the centers of the two modules. The dimer is about 77 Å in length, as measured along the particle axis (see Figure 8c). The diad between the C domains makes angles of 85, 90, 5, and 27° with the *a**, *b*, *c*, and particle axis directions. Chain segments related by the twofold axes can be compared in the stereo photographs in Figures 9 and 10.

The major phenolic (or *p*-hydroxymercuribenzenesulfonate) heavy-atom sites are related by the twofold axis between the V regions (see Table I and Figure 12b).

*Interactions between V and C Regions in the Two Monomers.* The distance between the centers of the intrachain disulfide bonds in the V and C domains of monomer 1 is 25 Å, and the corresponding distance in monomer 2 is 43 Å. This indicates a striking difference in the spatial relationships between the V and C domains in the two monomers.

The long axes of envelopes drawn around the V and C domains intersect in the switch region at an angle of approximately 70° (see Figure 8b). In monomer 2, the long dimensions of the V and C regions lie at an angle of ~110°. The sharp turn in monomer 1 occurs on the amino side of leucine 110.

One of the interactions appearing as continuous density at 6 Å involves the residue at position ~7 in the N-terminal segment and the main chain at valine 148 of monomer 1 (see Figure 7). The second occurs between the residue at position ~9 and the side chain of glutamic acid 202. These interactions

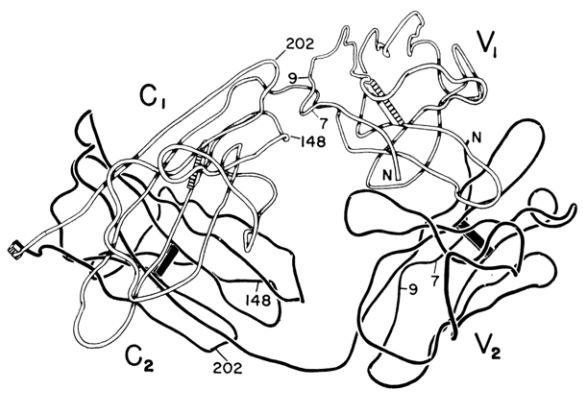


FIGURE 7: Tracing of a photograph of the model of the Bence-Jones dimer with the C domain of monomer 1 facing the camera. The cavity between the V domains is on the right and the interchain disulfide bond is on the left. This view shows the close proximity of the pairs of residues (9 and 202; 7 and 148) which interact in monomer 1; the corresponding pairs are widely separated in monomer 2.

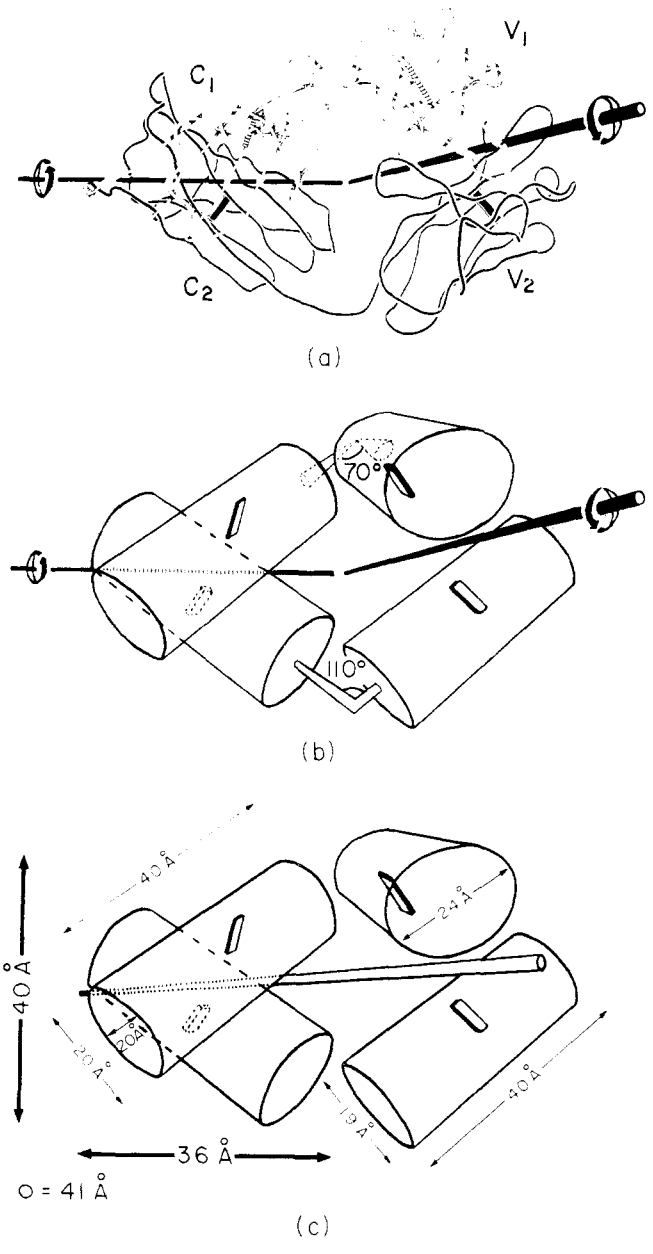


FIGURE 8: (a) Local pseudotwofold axes of rotation in the Bence-Jones dimer. This is the same view of the model as in Figure 7. The diad on the right runs through the center of the cavity between the V domains and intersects the twofold axis between the C domains at an angle of about 120°. (b) Schematic representation of the dimer. The long axes through the cylinders representing the $V_1$ and $C_1$ domains make an angle of about 70°; the corresponding angle in monomer 2 is ~110°. (c) Dimensions of the Bence-Jones dimer and its constituent domains. A "particle axis," defined as a line through the centers of the large and small modules, is included in the drawing. The length of the dimer, measured along this axis, is 77 Å. The thicker arrows indicate dimensions of the small module, as distinguished from individual domains. The third dimension of the small module is normal to the page, and is listed next to the open circle.

are impossible in monomer 2 because of the wide separation of the corresponding segments.

The V and C domains of monomer 1 are also closely situated at position 147, at which valine is substituted for alanine in the Mz λ chain (Milstein *et al.*, 1967). Substitutions in this site have to be limited to residues with small side chains if the structure is to be maintained. In monomer 2 position 147 is on the surface, with presumably no spatial restrictions on the nature of the side chain (see Figures 7 and 13).

An additional intrachain disulfide bond linking the V and C domains has been observed in rabbit light chains (Strosberg *et al.*, 1972). The corresponding residues are found at positions 82 and 174 in the Mcg λ chain, if homologies are assumed (see Figure 6). A disulfide bridging these residues is possible in monomer 2, but not in monomer 1. This implies that monomer 2 is a closer homolog to the rabbit light chains, and perhaps to light chains in general, than monomer 1. Such an implication leads to the further assumption that monomer 1 fills the structural role of the heavy chain in Fab fragments or in whole antibody molecules.

*Comparison of the V and C Regions.* The V and C regions bear a strong resemblance in overall shape and folding, as well as in the location of significant residues. The most characteristic feature of the C domain is the arrangement of chain segments in two distinct layers, which are 9–10 Å apart. There are four antiparallel chains in one layer and three antiparallel segments in the second layer, as shown schematically in Figure 11. In the V region the layers merge, since the N-terminal segment is not only a member of the four-chain layer, but also closely approaches one of the segments in the three-chain layer (see segments 1–14 and 96–112 in Figure 11).

For more detailed comparisons, the corresponding segments in the two halves can be considered homologous. The present V and C regions are under control of separate genes, but these are believed to be derived from a common primordial gene (Singer and Doolittle, 1966; Hill *et al.*, 1966; for reviews, see Milstein and Pink, 1970; Hood and Talmage, 1970). The V domain consists of 111 amino acid residues, of which 67 form the loop connected by the disulfide bond between half-cystine residues 22 and 90. In the C region of 105 residues, the homologous loop between half-cystines 138 and 197 contains 58 residues. The remainder of the molecule is composed of an N-terminal segment of 21 residues, a section of 47 residues connecting the intrachain loops, and a C-terminal segment of 19 residues.

In the four-chain layers, the first two antiparallel segments include residues 1–26 in the V region and residues 114–144 in the C domain (by strict homology the C segment should begin at residue 117). The centers of the bends between the segments occur at residues 14 and 131. The other pairs of segments consist of residues 61–82 and 161–190, with bends at residues 68 and 173.

In the three-chain layers one segment is composed of residues 32–42 in the V region and 145–155 in the C domain. The remaining pairs are made up of residues 83–110 and 191–216, with bends at residues 96 and 202.

The middle segment in the three-chain layer of each domain is connected to a parallel segment in the four-chain layer by the intrachain disulfide bond (see Figure 11). This arrangement places the disulfide bond in the center of the domain. One side of each disulfide bond is shielded by a tryptophan side chain: the "invariant" tryptophan (no. 37) in the V region (see Figure 4) and residue 152 in the C domain. The intrachain loop of each domain is on the same side of the disulfide bond as the tryptophan residue.

The segments and layers in the V region are more irregular than those in the C domain. Residues 48–60 are present in a highly irregular segment which makes several turns (see Figure 11). This segment, which includes the second hypervariable region, has no equivalent in the C domain. The loop representing residues 27–31 is also unique to the V domain

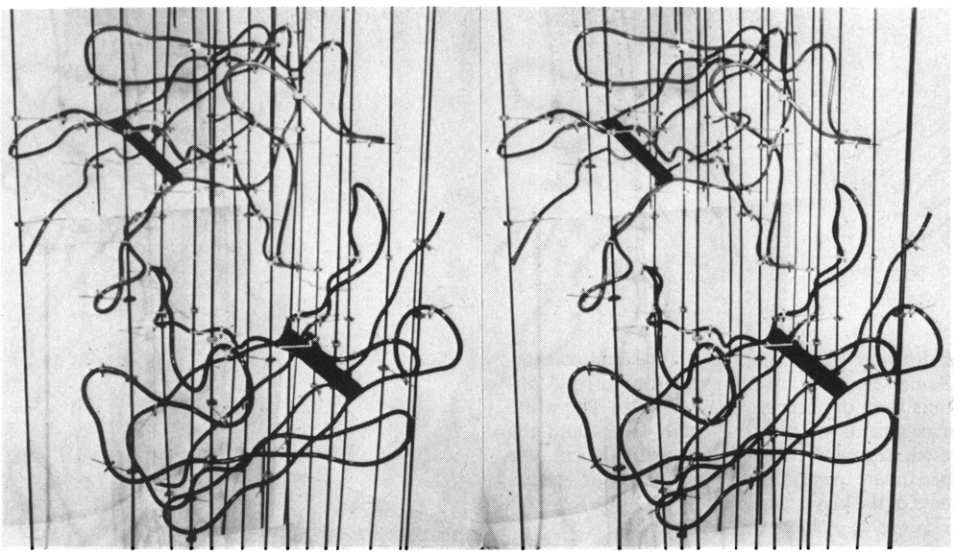

FIGURE 9: Photograph of the model of the V domains: stereo view approximately down the pseudotwofold axis. The hypervariable regions lining the cavity between the domains can be identified by comparison with the drawings in Figure 12. The accessibility of each N-terminus is clearly shown in this view.

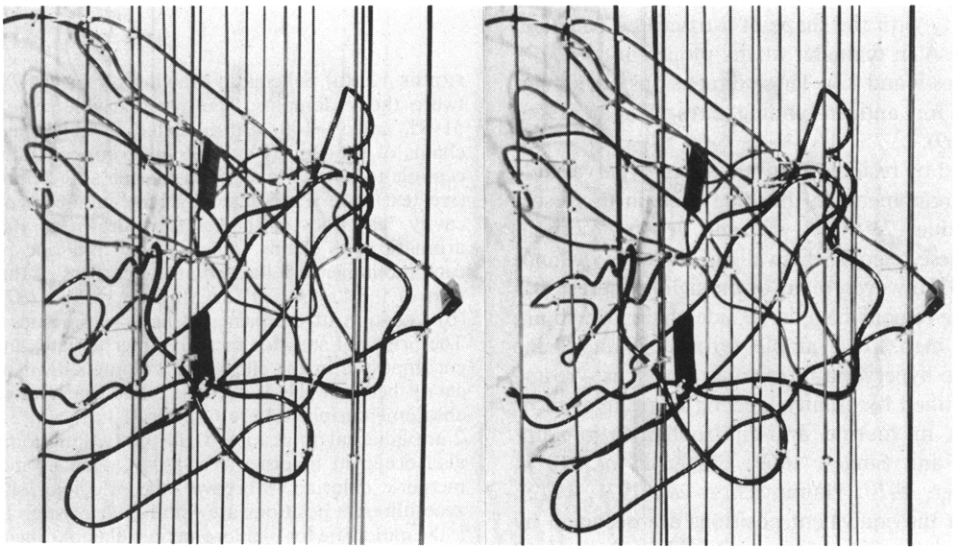

FIGURE 10: Stereo photograph of the model of the C domains in the same view as in Figure 6. Specific segments can be identified by reference to Figures 11 and 13. Note in particular the interacting surfaces along the four-chain layers of the two domains.

(see Figure 11). This loop is part of the first hypervariable region and contains residues which by their insertion or deletion partly determine the division of λ chains into subgroups (Putnam *et al.*, 1967a,b; Milstein and Pink, 1970; Garver and Hilschmann, 1971). In the figures this region appears as a loop only in monomer 2. The comparable segment of electron density in monomer 1 is low, and the structure shown represents the best fit to this density.

The appearance of the layers in the C regions is reminiscent of the "twisted sheet" of β structure noted in carboxypeptidase A (Lipscomb *et al.*, 1968). In the Bence-Jones dimer there are many examples in which the chains are separated by distances appropriate for hydrogen bonding (*i.e.*, ~5 Å), and model building is being initiated to assign the locations of such bonds. The C-terminal segments in adjacent dimers run antiparallel in the crystal, and probably form intermolecular hydrogen bonds (see boundary between dimers in Figure 3).

Circular dichroism (CD) spectra of light chains and their isolated domains, as well as whole antibodies and their Fab, Fc, and $C_H3$ fragments, have been used to estimate the amount of β structure (Cathou *et al.*, 1968; Ross and Jirgensons, 1968; Ghose and Jirgensons, 1971; Björk and Tanford, 1971; Cathou and Dorrington, 1973). Collectively, the CD results predict a larger amount of β structure in the C domain than in the V region of a light chain.

The four-chain layer in the C domain forms a concave surface, which is crossed diagonally by the complementary segments from a second monomer to give the X-shaped arrangement of chains seen in Figure 10. In the regions of close proximity, solvent appears to be excluded, and part of the interdomain space is occupied by large side chains.

The three-chain layers of the C domains supply the outside surfaces in the dimer. In striking contrast and counter to expectations based on homologies, the outer surfaces in the V regions are provided mainly by the four-chain layers. The three-chain layers face each other and form the interdomain cavity to be discussed in the next section. While the three-dimensional structures of the V and C domains support the

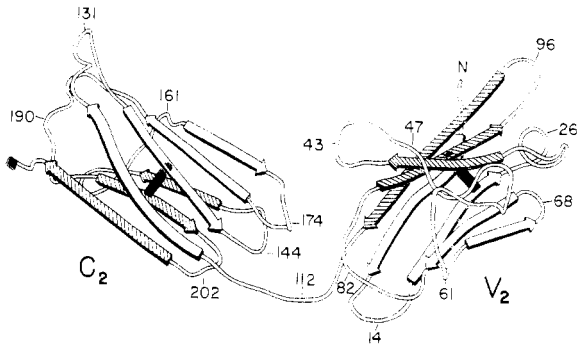


FIGURE 11: Schematic drawing of monomer 2, in the same orientation as in Figure 7. Some segments are represented by arrows, indicating chain directions but not accurate chain lengths. The white arrows correspond to segments of the four-chain layers and the striated arrows represent segments of the three-chain layers (see text for details). Approximate positions are presented for special residues and constituents of the bends.

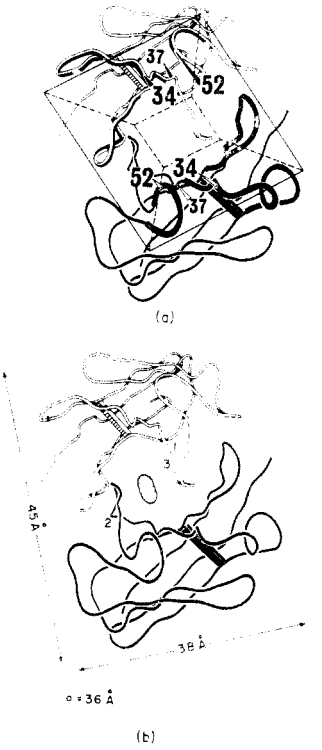


FIGURE 12: (a) Schematic drawing of the view into the cavity between the V domains. The hypervariable regions (residues 23–36, 51–55, and 91–100) are indicated by thickened chains. The side chains of residues 34 and 52, in positions equivalent to those susceptible to affinity labeling in murine anti-dinitrophenyl antibodies (see text), are represented by large numbers protruding into the cavity. The floor of the cavity is shown as a square array. Four aromatic side chains, one tyrosine and one phenylalanine from each monomer, are located at the corners of the square. The position of the "invariant" tryptophan residue (37) is also indicated. (b) Location of the principal heavy-atom sites in the V domains. The principal sites for mersalyl, merthiolate, and mercuhydrin are encompassed in the ellipsoidal volume shown schematically in the cavity between the V domains. The major and minor sites of *o*-chloromercuriphenol are numbered 1, 2, and 3. Major sites 1 and 2 are adjacent to residue 41 in the two monomers. These sites are also occupied in other derivatives, such as mersalyl and methylmercuric chloride. Moreover, the principal *p*-hydroxymercuribenzenesulfonate positions are within 5 Å of sites 1 and 2. Location 3 is the minor site for *o*-chloromercuriphenol. The arrows indicate two dimensions of the large module. The third dimension is normal to the page, and is listed next to the open circle.

hypothesis of a common ancestral gene, the functions of key homologous segments seem to have diverged markedly during evolution.

*Cavity between the V Domains.* The V regions are partially separated by a cavity with the shape of a truncated cone and dimensions of ~15 Å in diameter at the mouth and ~10 Å in depth (see Figures 9 and 12). These dimensions are similar to those deduced for antigen-binding sites (Kabat, 1966; Hsia and Piette, 1969).

The cavity is lined by residues from the three hypervariable segments of both monomers. In the Mcg λ chain these segments include residues 23–36, 51–55, and 91–100. Without the sequences of these regions, the walls of the cavity cannot be mapped in detail. However, many of the significant residues in the hypervariable regions have large side chains which are visible in the 3.5-Å map. For example, tyrosine 34 and lysine 54 from the first two hypervariable regions, as well as tyrosine 86, have been identified by affinity labeling as residues in or near binding sites in murine anti-dinitrophenyl immunoglobulins (Thorpe and Singer, 1969; Singer *et al.*, 1971; Goetzl and Metzger, 1970; Haimovich *et al.*, 1971, 1972). In the Mcg protein the equivalent positions are occupied by residues 34, 52, and 88. Side chains of residues 34 and 52 protrude into the cavity (see Figure 12a), but residue 88 is directed away from the cavity toward the interior of each V region (see Figure 3). Similarly, the invariant tryptophan residue (37) cannot be directly involved in the binding of antigens, since its side chain also points away from the cavity (see Figures 4 and 12a).

The section between residue 33 and tryptophan 37 in each monomer acts as part of the walls of the cavity. The floor of the cavity is formed by an array of four aromatic side chains, one tyrosine and phenylalanine from each monomer (see Figures 4 and 12a). The tyrosine has been identified as residue 38, which may be replaced by phenylalanine or histidine in other human λ chains (Garver and Hilschmann, 1971).

The general locations of the heavy-atom binding sites within the cavity are illustrated in Figure 12b. Mersalyl was found in two sites, major and minor, which appear superimposed in the view presented in Figure 12b. Because of spatial restrictions, it is unlikely that the two sites are occupied simultaneously in one molecule. However, there is sufficient space for a mersalyl ion to assume different orientations, and this freedom of movement is manifest in a high temperature factor. Mercuhydrin occupies a site centered between the two mersalyl positions. Merthiolate was found in the mersalyl sites, but with the major site corresponding to the minor mersalyl position and vice versa.

The combined structural features discussed in this section, together with the homologies of light and heavy chains, indicate that the cavity is probably the counterpart of an antigen-binding site in the Fab region of a functional antibody molecule.

*Accessibility of Specific Residues.* The properties of amino acid residues important for the structure or biological activity of light chains in solution were correlated with their positions in the three-dimensional structure of the Bence-Jones dimer. Among the residues considered were the termini, the side chains acting as antigenic determinants or genetic markers, and residues susceptible to chemical modification.

Both the N- and C-terminal segments were found on the surface of the dimer in positions exposed to solvent (see

Figure 6). The monomer does not have a free α-amino group because of cyclization of the N-terminal glutamine residue to pyrrolidonecarboxylic acid. The work of Milstein *et al.* (1972) suggests that glutamine may not have been the N-terminus of the protein as synthesized. They reported that κ chains were produced in certain cell-free systems as slightly larger precursors, which were subsequently cleaved near the amino end. Cleavage of such a precursor extension appears sterically feasible in the Mcg protein.

Although relatively constant, the sequences of the C halves in human λ chains vary in at least four locations, the two Mz sites, the Kern position, and the Oz antigenic locus. The first Mz substitution (valine for alanine 147; Milstein *et al.*, 1967) was discussed in relation to possible interactions between the V and C domains. The second replacement site (lysine for asparagine 174) is found on an exposed loop in both monomers of the Mcg protein (see Figure 13). The Kern position (156), in which glycine is substituted for serine (Ponstingl *et al.*, 1967; Hess *et al.*, 1971), and the Oz locus, associated with an arginine–lysine interchange at position 193 (Appella and Ein, 1967), are located on the surface of adjacent loops (see Figure 13).

Differences observed in antigenic properties of human κ chains by McLaughlin and Solomon (1972) were attributed to residues 9, 45, and 94–96. The comparable side chains in the Mcg λ chain are accessible to solvent.

Seon *et al.* (1969, 1971) correlated the reactivity of tyrosine and histidine side chains to iodination with their accessibility in a human (Col) κ chain. Tyrosines 49, 91, and 173 were accessible by this criterion; residues 36, 96, 140, 186, and 192 were less reactive; and tyrosine 87 was "buried." Of the two histidines, residue 198 was more reactive than 189. These results are generally consistent with the surroundings of the corresponding residues in the Mcg λ chain. In particular, the "buried" tyrosine residues (Mcg 89 = Col 87) in the two monomers occupy part of the interface between the V regions (see Figure 3). The pair of tyrosine residues (38) equivalent to Col 36 are constituents of the floor of the binding cavity (see Figure 3). Histidine 192 (Col 189) is on the surface of the molecule adjacent to arginine 193 of the Oz locus (see Figure 13), while histidine 201 (Col 198) is involved in the turn leading to the C-terminal 14 residues (see Figure 3). The side chain of histidine 201 appears to be less accessible than residue 192.

*Comparison of Mcg Bence-Jones Dimer with Light Chains in Myeloma Proteins or Antibody Molecules.* In the Mcg myeloma protein, the internal structure of each domain in the light chain is expected to be similar to that in the Bence-Jones molecule. However, the crystallographic twofold axis in the Mcg myeloma protein (Edmundson *et al.*, 1970) requires the spatial relations between the V and C regions to be identical in the two light chains.

Covalently linked light chains are also found in the Am(2)+ allotype of IgA2 proteins (Grey *et al.*, 1968; Jerry *et al.*, 1970; Tomasi and Grey, 1972). In these special cases, as in the usual IgG proteins, the noncovalent interactions between light and heavy chains predominate over interactions between light chains (Dorrington and Tanford, 1970; Tomasi and Grey, 1972; Cathou and Dorrington, 1973). If the interlight chain disulfide bond is reduced and alkylated, for example, the IgA2 proteins can be dissociated under mild conditions into half-molecules of light and heavy chains, rather than light chain dimers.

The assembly of normal IgG proteins probably requires monomers of light chains, since covalently linked dimers do not recombine with heavy chains (Stevenson and Dorrington, 1970). However, covalent light chain dimers have been found in reconstituted IgG proteins in which the usual disulfide bonds between light and heavy chains are not possible (Grey, 1969). If these findings are applicable to the Mcg myeloma protein, the C-terminal segments of the light chains can approach each other sufficiently close to form an interchain disulfide bond in the presence of heavy chains, without affecting the symmetry between half-molecules.

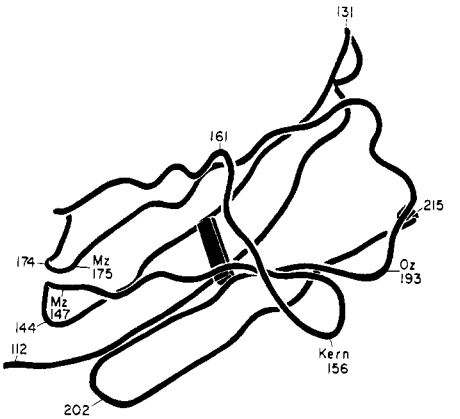


FIGURE 13: Tracing of the $C_2$ domain in the same orientation as in Figure 6. The sites at which amino acid substitutions are known to occur in human λ chains are marked as the two Mz, the Kern, and the Oz sites (consult text for details). Other residue positions are included for comparisons with Figure 11.

*Binding of Antigens or Haptens by Light Chains Alone.* Light chains separated from the heavy chains of functional antibodies may interact with the specific antigen or hapten in some cases. Mangalo *et al.* (1966) reported that light chain dimers from horse antibodies to diphtheria toxoid had 15% of the activity of the intact antibodies. Painter *et al.* (1972a) presented evidence for one binding site per dimer of light chains obtained from rabbit anti-dinitrophenyl, but the affinity for the hapten was low. Stevenson (1973) found that dimers, but not monomers, of renatured light chains bound Dnp or Methyl Orange haptens. The level of specific binding again was low when compared with the parent antibody. It is difficult to surmize whether the renaturation and dimerization steps in the preceding work led to molecules interacting to the extent seen in the covalently linked Mcg Bence-Jones dimer.

Although detailed binding studies have not been performed with the Mcg protein, the three-dimensional structure shows that the two V regions form a cavity which has many properties attributed to an antigen-binding site. In this structure one of the light chains simulates the heavy chain in an Fab fragment.

## Acknowledgments

We thank H. F. Deutsch for his continued interest and for collecting the urine samples from which the Bence-Jones protein was prepared; W. R. Cole, B. S. Kotula, W. J. Eisler, and D. A. Lebuis for design, construction, and maintenance of crystallographic equipment; G. E. Mikota, V. McCathren, and J. Moritz for building the optical comparator, with special guidance from W. R. Cole and J. W. Harrison; M. D. Fausch and F. A. Westholm for aid in preparing the electron density map; R. H. Bernard, L. E. Gorney, and A. Meyers for assistance with the figures; K. D. Hardman and C. F. Ainsworth for discussions; and S. S. Danyluk and J. F. Thomson for manuscript criticism.

References


Adams, M. J., Haas, D. J., Jeffery, B. A., McPherson, A., Jr., Mermall, H. L., Rossmann, M. G., Schevitz, R. W., and Wonacott, A. J. (1969), *J. Mol. Biol. 41*, 159.

Appella, E., and Ein, D. (1967), *Proc. Nat. Acad. Sci. U. S. 57*, 1449.

Björk, I., Karlsson, F. A., and Berggård, I. (1971), *Proc. Nat. Acad. Sci. U. S. 68*, 1707.

Björk, I., and Tanford, C. (1971), *Biochemistry 10*, 1280.

Blow, D. M., and Crick, F. H. C. (1959), *Acta Crystallogr. 12*, 794.

Capra, J. D. (1971), *Nature (London), New Biol. 230*, 61.

Capra, J. D., Kehoe, J. M., Winchester, R. J., and Kunkel, H. G. (1971), *Ann. N. Y. Acad. Sci. 190*, 371.

Cathou, R. E., and Dorrington, K. J. (1973), *in* Subunits in Biological Systems, Part C, Timasheff, S. N., and Fasman, G. D., Ed., New York, N. Y., Marcel Dekker (in press).

Cathou, R. E., Kulczycki, A., Jr., and Haber, E. (1968), *Biochemistry 7*, 3958.

Cebra, J. J., Ray, A., Benjamin, D., and Birshtein, B. (1971), *Progr. Immunol., Int. Congr. Immunol., 1st*, 269.

Cullis, A. F., Muirhead, H., Perutz, M. F., Rossmann, M. G., and North, A. C. T. (1962), *Proc. Roy. Soc., Ser. A 265*, 161.

Dayhoff, M. O., Ed. (1972), Atlas of Protein Sequence and Structure, Vol. V, Silver Spring, Md., National Biomedical Research Foundation, p D-256.

Deutsch, H. F. (1971), *Seibutsu Butsuri Kagaku 16*, 73.

Deutsch, H. F., and Suzuki, T. (1971), *Ann. N. Y. Acad. Sci. 190*, 472.

Dickerson, R. E., Eisenberg, D., Varnum, J., and Kopka, M. L. (1969), *J. Mol. Biol. 45*, 77.

Dickerson, R. E., Kendrew, J. C., and Strandberg, B. E. (1961), *Acta Crystallogr. 14*, 1188.

Dickerson, R. E., Weinzierl, J. E., and Palmer, R. A. (1968), *Acta Crystallogr., Sect. B 24*, 997.

Dorrington, K. J., and Tanford, C. (1970), *Advan. Immunol. 12*, 333.

Edelman, G. M., and Gall, W. E. (1969), *Annu. Rev. Biochem. 38*, 415.

Edelman, G. M., and Gally, J. A. (1962), *J. Exp. Med. 116*, 207.

Edmundson, A. B., Schiffer, M., Ely, K. R., and Wood, M. K. (1972), *Biochemistry 11*, 1822.

Edmundson, A. B., Schiffer, M., Wood, M. K., Hardman, K. D., Ely, K. R., and Ainsworth, C. F. (1971), *Cold Spring Harbor Symp. Quant. Biol. 36*, 427.

Edmundson, A. B., Wood, M. K., Schiffer, M., Hardman, K. D., Ainsworth, C. F., Ely, K. R., and Deutsch, H. F. (1970), *J. Biol. Chem. 245*, 2763.

Ely, K. R., Girling, R. L., Schiffer, M., Cunningham, D. E., and Edmundson, A. B. (1973), *Biochemistry* (in press).

Epp, O., Palm, W., Fehlhammer, H., Ruhlmann, A., Steigemann, W., Schwager, P., and Huber, R. (1972), *J. Mol. Biol. 69*, 315.

Fett, J. W., Deutsch, H. F., and Smithies, O. (1973), *Immunochemistry 10*, 115.

Franěk, F. (1971), *Eur. J. Biochem. 19*, 176.

Fraser, K. J., Poulsen, K., and Haber, E. (1972), *Biochemistry 11*, 4974.

Garver, F. A., and Hilschmann, N. (1971), *FEBS (Fed. Eur. Biochem. Soc.) Lett. 16*, 128.

Ghose, A. C., and Jirgensons, B. (1971), *Biochim. Biophys. Acta 251*, 14.

Goetzl, E. J., and Metzger, H. (1970), *Biochemistry 9*, 3862.

Grey, H. M. (1969), *J. Immunol. 102*, 848.

Grey, H. M., Abel, C. A., Yount, W. J., and Kunkel, H. G. (1968), *J. Exp. Med. 128*, 1223.

Haimovich, J., Eisen, H. N., and Givol, D. (1971), *Ann. N. Y. Acad. Sci. 190*, 352.

Haimovich, J., Eisen, H. N., Hurwitz, E., and Givol, D. (1972), *Biochemistry 11*, 2389.

Hess, M., Hilschmann, N., Rivat, L., Rivat, C., and Ropartz, C. (1971), *Nature (London), New Biol. 234*, 58.

Hill, R. L., Delaney, R., Fellows, R. E., Jr., and Lebovitz, H. E. (1966), *Proc. Nat. Acad. Sci. U. S. 56*, 1762.

Hilschmann, N., and Craig, L. C. (1965), *Proc. Nat. Acad. Sci. U. S. 53*, 1403.

Hood, L., and Talmage, D. W. (1970), *Science 168*, 325.

Hsia, J. C., and Piette, L. H. (1969), *Arch. Biochem. Biophys. 129*, 296.

Inbar, D., Hochman, J., and Givol, D. (1972), *Proc. Nat. Acad. Sci. U. S. 69*, 2659.

Jerry, L. M., Kunkel, H. G., and Grey, H. M. (1970), *Proc. Nat. Acad. Sci. U. S. 65*, 557.

Kabat, E. A. (1966), *J. Immunol. 97*, 1.

Kabat, E. A., and Wu, T. T. (1971), *Ann. N. Y. Acad. Sci. 190*, 382.

Karlsson, F. A., Peterson, P. A., and Berggård, I. (1969), *Proc. Nat. Acad. Sci. U. S. 64*, 1257.

Karlsson, F. A., Peterson, P. A., and Berggård, I. (1972), *J. Biol. Chem. 247*, 1065.

Kehoe, J. M., and Capra, J. D. (1971), *Proc. Nat. Acad. Sci. U. S. 68*, 2019.

Lipscomb, W. N., Hartsuck, J. A., Reeke, G. N., Jr., Quiocho, F. A., Bethge, P. H., Ludwig, M. L., Steitz, T. A., Muirhead, H., and Coppola, J. C. (1968), *Brookhaven Symp. Biol. 21*, 24.

Mangalo, R., Iscaki, S., and Raynaud, M. (1966), *C. R. Acad. Sci., Ser. D 263*, 204.

McLaughlin, C. L., and Solomon, A. (1972), *J. Biol. Chem. 247*, 5017.

Milstein, C., Brownlee, G. G., Harrison, T. M., and Mathews, M. B. (1972), *Nature (London), New Biol. 239*, 117.

Milstein, C., Frangione, B., and Pink, J. R. L. (1967), *Cold Spring Harbor Symp. Quant. Biol. 32*, 31.

Milstein, C., and Pink, J. R. L. (1970), *Progr. Biophys. Mol. Biol. 21*, 209.

Osserman, E. F., Takatsuki, K., and Talal, N. (1964), *Semin. Hematol. 1*, 3.

Padlan, E. A., Segal, D. M., Spande, T. F., Davies, D. R., Rudikoff, S., and Potter, M. (1973), *Nature (London), New Biol.* (in press).

Painter, R. G., Sage, H. J., and Tanford, C. (1972a), *Biochemistry 11*, 1327.

Painter, R. G., Sage, H. J., and Tanford, C. (1972b), *Biochemistry 11*, 1338.

Poljak, R. J., Amzel, L. M., Avey, H. P., Becka, L. N., and Nisonoff, A. (1972), *Nature (London), New Biol. 235*, 137.

Ponstingl, H., Hess, M., Langer, B., Steinmetz-Kayne, M., and Hilschmann, N. (1967), *Hoppe-Seyler's Z. Physiol. Chem. 348*, 1214.

Porter, R. R. (1971), *Harvey Lect. 65*, 157.

Press, E. M., Fleet, G. W. J., and Fisher, C. E. (1971), *Progr. Immunol., Int. Congr. Immunol., 1st*, 234.

Putnam, F. W., Shinoda, T., Titani, K., and Wikler, M. (1967a), *Science 157*, 1050.

Putnam, F. W., Titani, K., Wikler, M., and Shinoda, T. (1967b), *Cold Spring Harbor Symp. Quant. Biol. 32*, 9.

Richards, F. M. (1968), *J. Mol. Biol. 37*, 225.

Ross, D. L., and Jirgensons, B. (1968), *J. Biol. Chem. 243*, 2829.
Sarma, V. R., Silverton, E. W., Davies, D. R., and Terry, W. D. (1971), *J. Biol. Chem. 246*, 3753.
Schiffer, M., Hardman, K. D., Wood, M. K., Edmundson, A. B., Hook, M. E., and Ely, K. R. (1970), *J. Biol. Chem. 245*, 728.
Schramm, H. J. (1971), *Hoppe-Seyler's Z. Physiol. Chem. 352*, 1134.
Seon, B.-K., Roholt, O. A., and Pressman, D. (1969), *Biochim. Biophys. Acta 194*, 397.
Seon, B.-K., Roholt, O. A., and Pressman, D. (1971), *J. Biol. Chem. 246*, 887.
Shotton, D. M., and Watson, H. C. (1970), *Phil. Trans. Roy. Soc. London, Ser. B 257*, 111.
Singer, S. J., and Doolittle, R. F. (1966), *Science 153*, 13.
Singer, S. J., Martin, N., and Thorpe, N. O. (1971), *Ann. N. Y. Acad. Sci. 190*, 342.
Solomon, A., and McLaughlin, C. L. (1969), *J. Biol. Chem. 244*, 3393.
Solomon, A., McLaughlin, C. L., Wei, C. H., and Einstein, J. R. (1970), *J. Biol. Chem. 245*, 5289.
Stevenson, G. T. (1973), *Biochem. J.* (in press).
Stevenson, G. T., and Dorrington, K. J. (1970), *Biochem. J. 118*, 703.
Strosberg, A. D., Fraser, K. J., Margolies, M. N., and Haber, E. (1972), *Biochemistry 11*, 4978.
Thorpe, N. O., and Singer, S. J. (1969), *Biochemistry 8*, 4523.
Titani, K., Whitley, E., Jr., and Putnam, F. W. (1966), *Science 152*, 1513.
Tomasi, T. B., and Grey, H. M. (1972), *Progr. Allergy 16*, 81.
Wikler, M., and Putnam, F. W. (1970), *J. Biol. Chem. 245*, 4488.
Wu, T. T., and Kabat, E. A. (1970), *J. Exp. Med. 132*, 211.
Wyckoff, H. W., Doscher, M., Tsernoglou, D., Inagami, T., Johnson, L. N., Hardman, K. D., Allewell, N. M., Kelly, D. M., and Richards, F. M. (1967), *J. Mol. Biol. 27*, 563.

# Extrinsic Cotton Effects in Retinaldehyde Schiff's Bases†

Edward M. Johnston and Robert Zand*

ABSTRACT: Schiff's bases have been synthesized from *all-trans*-retinaldehyde and (*S*)-α-phenylethylamine, *S*-α-(1-naphthyl)-ethylamine, *R*-(+)-2,2′-dimethyl-6,6′-diaminobiphenyl, and poly-L-lysine. The Schiff's base of 11-*cis*-retinaldehyde with (*S*)-α-(1-naphthyl)ethylamine was also prepared. The absorption and circular dichroic spectra were measured for the parent compound and the protonated forms over the wavelength region of 190–700 nm. Extrinsic Cotton effects were observed in the region of the major retinaldehyde absorption band centered at about 360 nm. Protonation of the Schiff's base caused the absorption and circular dichroism band to shift to about 410 nm. The Schiff's base, $N^{\epsilon}$-*all-trans*-retinylidene-L-lysine and *N*-*all-trans*-retinylidene-L-dipalmitoylphosphatidylethanolamine did not exhibit extrinsic Cotton effects in the region of retinaldehyde absorption. The results are pertinent to the origins of the observed Cotton effect in the visible wavelength region of rhodopsin.

The visual pigment rhodopsin exhibits a broad circular dichroic (CD) band in the region of 500 nm where the 11-*cis*-retinaldehyde component of rhodopsin has an absorption maximum. *all-trans*- and 11-*cis*-retinaldehyde are optically inactive molecules and the mechanism for the induction of the optical activity as well as the significance of the problem relative to the structure of rhodopsin is an unsolved problem.

In 1966, the CD spectrum of bovine rhodopsin was reported (Crescitelli *et al.*, 1966). The initial explanation that was considered and then rejected by these workers was that the optical activity arose from an extrinsic mechanism. The explanation advanced for the induction of optical activity into the retinaldehyde chromophore was based on the hypothesis that the binding of 11-*cis*-retinaldehyde to opsin was accompanied by a twisting of the aldehyde into an asymmetric conformation. The twisted chromophore concept was developed further (Mommaerts, 1969) by suggesting that 11-*cis*-retinaldehyde could exist in two enantiomeric forms (Figure 1). When the 11-*cis*-retinaldehyde is bound to opsin one enantiomer was thought to be preferentially stabilized and "frozen in" thereby providing the asymmetry necessary for optical activity. The concept of intrinsic optical activity in the retinaldehyde portion of rhodopsin has recently been treated more extensively (Honig *et al.*, 1973).

The extrinsic mechanism was reintroduced by Kito *et al.* (1968) to explain the observed Cotton effects in squid rhodopsin. This approach was developed further by Johnston and Zand (1972) and Waggoner and Stryer (1971). In this mechanism the optical activity may arise through a Kirkwood-type coupled oscillator mechanism (Kirkwood, 1937) so that the retinaldehyde transitions may become optically active by coupling with the transitions of nearby aromatic side chains.

The present study was undertaken with the view that spectral studies of Schiff's bases (Table I) derived from retinaldehyde and appropriate optically active amines would provide information that would help to establish the mecha-

† From the Biophysics Research Division, Institute of Science and Technology, and Department of Biological Chemistry, University of Michigan, Ann Arbor, Michigan 48105. *Received February 9, 1973.* This work includes material from a thesis submitted by E. M. J. in partial fulfillment of the requirements for the degree of Doctor of Philosophy. A preliminary report of this work has been published (Johnston and Zand, 1972). Supported in part by National Institutes of Health Grants NB-05036 GM-1355 and GM-14035.